HISTONE DEACETYLASE6 Interacts with FLOWERING LOCUS D and Regulates Flowering in Arabidopsis[1][C][W][OA]

Chun-Wei Yu, Xuncheng Liu, Ming Luo, Chiayang Chen, Xiaodong Lin, Gang Tian, Qing Lu, Yuhai Cui, and Keqiang Wu*

Institute of Plant Biology, College of Life Science, National Taiwan University, Taipei 106, Taiwan (C.-W.Y., X.L., M.L., C.C., K.W.); Key Laboratory of Plant Resources Conservation and Sustainable Utilization, South China Botanical Garden, Chinese Academy of Sciences, Guangzhou 510650, China (M.L.); School of Life Science, Sun Yat-Sen University, Guangzhou 510275, China (X.L.); and Southern Crop Protection and Food Research Centre, Agriculture and Agri-Food Canada, London, Ontario, Canada N5V 4T3 (G.T., Q.L., Y.C.)

Histone acetylation and deacetylation play an important role in epigenetic controls of gene expression. HISTONE DEACETYLASE6 (HDA6) is a REDUCED POTASSIUM DEPENDENCY3-type histone deacetylase, and the Arabidopsis (*Arabidopsis thaliana*) *hda6* mutant *axe1-5* displayed a late-flowering phenotype. *axe1-5/flc-3* double mutants flowered earlier than *axe1-5* plants, indicating that the late-flowering phenotype of *axe1-5* was *FLOWERING LOCUS C* (*FLC*) dependent. Bimolecular fluorescence complementation, in vitro pull-down, and coimmunoprecipitation assays revealed the protein-protein interaction between HDA6 and the histone demethylase FLD. It was found that the SWIRM domain in the amino-terminal region of FLD and the carboxyl-terminal region of HDA6 are responsible for the interaction between these two proteins. Increased levels of histone H3 acetylation and H3K4 trimethylation at *FLC*, *MAF4*, and *MAF5* were found in both *axe1-5* and *fld-6* plants, suggesting functional interplay between histone deacetylase and demethylase in flowering control. These results support a scenario in which histone deacetylation and demethylation cross talk are mediated by physical association between HDA6 and FLD. Chromatin immunoprecipitation analysis indicated that HDA6 bound to the chromatin of several potential target genes, including *FLC* and *MAF4*. Genome-wide gene expression analysis revealed that, in addition to genes related to flowering, genes involved in gene silencing and stress response were also affected in *hda6* mutants, revealing multiple functions of HDA6. Furthermore, a subset of transposons was up-regulated and displayed increased histone hyperacetylation, suggesting that HDA6 can also regulate transposons through deacetylating histone.

In eukaryotic cells, gene activity is controlled not only by DNA sequences but also by epigenetic marks, which can be transmitted to a cell's progeny during mitosis or meiosis. Epigenetic changes involve the modification of DNA activity by methylation, histone modifications, or chromatin remodeling without alteration of the nucleotide sequence (Berger, 2007). Histone modifications include acetylation, methylation, phosphorylation, ubiquitination, sumoylation, and ADP ribosylation. The functional consequences of histone modifications can be direct, causing structural changes to chromatin, or indirect, acting through the recruitment of effector proteins. All histone modifications are removable, which may provide a versatile way for regulating gene expression during plant development and the plant response to environmental stimuli. The reversible acetylation and deacetylation of specific Lys residues on core histone N-terminal tails is catalyzed by histone acetyltransferases and deacetylases (HDAs or HDACs; Pandey et al., 2002; Chen and Tian, 2007). The action of both enzymes generates patterns of acetylation that may specify downstream biological processes such as transcriptional regulation. In general, hyperacetylated histones are associated with gene activation, whereas hypoacetylated histones are related to gene repression. Although histone acetylation is an integral part of transcriptional regulatory systems, little is known regarding its physiological roles and downstream target genes in plants.

More recent studies indicated that histone modifications including acetylation are involved in plant flowering (He and Amasino, 2005; Dennis and Peacock, 2007). In Arabidopsis (*Arabidopsis thaliana*), flowering time is controlled by several pathways, including the photoperiod, gibberellin, autonomous, and vernalization pathways (Boss et al., 2004; Henderson and Dean, 2004). FLOWERING LOCUS C (FLC) is a key regulator of flowering, which negatively regulates downstream flowering activators such as *FT* and

[1] This work was supported by the National Science Council of Taiwan (grant nos. 97–2311–B–002–004–MY3, 98–2628–B–002–016–MY3, and 99–2321–B–002–027–MY3) and the National Taiwan University (grant nos. 98R0066–36 and 99R80840).

* Corresponding author; e-mail kewu@ntu.edu.tw.

The author responsible for distribution of materials integral to the findings presented in this article in accordance with the policy described in the Instructions for Authors (www.plantphysiol.org) is: Keqiang Wu (kewu@ntu.edu.tw).

[C] Some figures in this article are displayed in color online but in black and white in the print edition.

[W] The online version of this article contains Web-only data.

[OA] Open Access articles can be viewed online without a subscription.

www.plantphysiol.org/cgi/doi/10.1104/pp.111.174417

SOC1 (Michaels and Amasino, 2001; Helliwell et al., 2006). High expression of *FLC* results in a delayed-flowering phenotype. In the autonomous mutant *fld*, *FLC* displays hyperacetylation of histone H3 and H4, and it is proposed that FLD might participate in the deacetylation of *FLC* chromatin as a component of a HDAC complex (He et al., 2003). *FLD* encodes a plant ortholog of the human protein Lys-Specific Demethylase1 (LSD1) that is involved in H3K4 demethylation (Jiang et al., 2007). However, the histone deacetylase activity associated with FLD is unknown. Our previous studies demonstrated that the *Arabidopsis HISTONE DEACETYLASE6* (*HDA6*) mutant, *axe1-5*, and *HDA6*-RNAi (for RNA interference) plants displayed a delayed-flowering phenotype (Wu et al., 2008). Furthermore, *FLC* was up-regulated and hyperacetylated in *axe1-5* and *HDA6*-RNAi plants, suggesting that HDA6 may regulate flowering by repressing *FLC* expression.

In this study, we further investigate the function of HDA6 and its interaction with FLD. Bimolecular fluorescence complementation (BiFC), in vitro pull-down, and coimmunoprecipitation assays revealed direct protein-protein interaction between HDA6 and FLD, suggesting that they could act together in a protein complex. Increased levels of histone H3 acetylation and H3K4 trimethylation in *FLC*, *MAF4*, and *MAF5* were found in both *axe1-5* and *fld-6* plants, indicating functional interplay between histone deacetylase and demethylase through HDA6 and FLD interaction in flowering control.

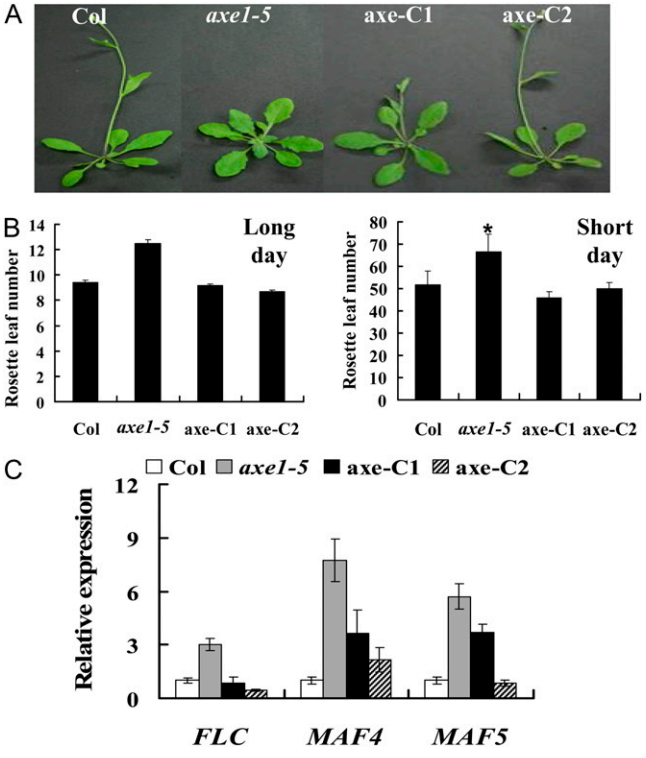

Figure 1. Complementation of the late-flowering phenotype of *axe1-5* by overexpressing *35S:HDA6-FLAG*. A, *axe1-5* and the complementation lines (axe-C1 and axe-C2) grown under LD conditions compared with the Col wild type. B, Rosette leaf numbers at bolting of Col, *axe1-5*, axe-C1, and axe-C2 plants grown under LD and SD conditions. At least 20 plants were scored for each line. Error bars indicate SD. * Under SD conditions, most *axe1-5* plants did not flower 120 d after germination, and the rosette leaf number was counted at 120 d. C, qRT-PCR analysis of the expression of *FLC*, *MAF4*, and *MAF5* in Col, *axe1-5*, axe-C1, and axe-C2 plants grown under LD conditions for 20 d. [See online article for color version of this figure.]

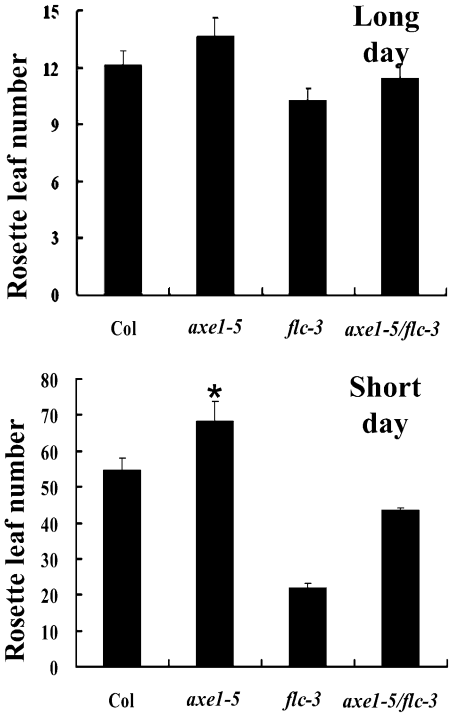

Figure 2. *FLC*-dependent late flowering in *axe1-5*. Rosette leaf numbers at bolting of Col, *axe1-5*, *flc-3*, and *axe1-5/flc-3* plants grown under LD and SD conditions are shown. Error bars indicate SD. At least 20 plants were scored for each line. * Under SD conditions, most *axe1-5* plants did not flower 120 d after germination, and the rosette leaf number was counted at 120 d.

RESULTS

The Late-Flowering Phenotype of *axe1-5* Is *FLC* Dependent

Previously, we reported that the Arabidopsis *HDA6* mutant, *axe1-5*, displayed a late-flowering phenotype (Wu et al., 2008). To confirm that the delayed-flowering phenotype was indeed caused by the *HDA6* mutation in *axe1-5* plants, a *35S*::*HDA6-FLAG* transgene was introduced into *axe1-5* plants by *Agrobacterium tumefaciens*-mediated transformation (Clough and Bent, 1998). Two independent transgenic lines, axe-C1 and axe-C2, expressing *35S*::*HDA6-FLAG* were generated. Both axe-C1 and axe-C2 plants expressing the trans-

gene flowered earlier than *axe1-5* plants (Fig. 1, A and B). In addition, the expression of *FLC*, *MAF4*, and *MAF5* was decreased in the axe-C1 and axe-C2 plants (Fig. 1C). Rescue of the delayed-flowering phenotype of *axe1-5* plants by expression of the *35S*::*HDA6-FLAG* transgene suggests that the delayed-flowering phenotype of *axe1-5* plants is indeed due to the *HDA6* mutation.

FLC is a major transcription repressor in the transition from vegetative growth to reproductive development stages (Michaels and Amasino, 2001). To investigate whether the delayed-flowering phenotype of *axe1-5* was dependent on high *FLC* expression, we generated the *axe1-5/flc-3* double mutant. *axe1-5/flc-3* double mutants flowered earlier than *axe1-5* plants both under long-day (LD) and short-day (SD) conditions (Fig. 2), indicating that the late-flowering phenotype of *axe1-5* was *FLC* dependent. However, *axe1-5/flc-3* plants flowered later than *flc-3* single mutant plants, suggesting that a portion of the late-flowering phenotype of *axe1-5* mutants could be due to other floral repressors (Deng et al., 2007). Consistent with this hypothesis, the expression of two additional MADS box genes in the *FLC* clade, *MAF4* and *MAF5*, was also up-regulated in *axe1-5* mutants (Fig. 1C).

Histone H3 Acetylation and H3K4 Trimethylation Levels of *FLC*, *MAF4*, and *MAF5* Are Increased in *axe1-5* and *fld-6* Plants

To analyze whether the higher expression of *FLC*, *MAF4*, and *MAF5* in *axe1-5* mutants is related to histone hyperacetylation in the chromatins, a chromatin immunoprecipitation (ChIP) assay was used to analyze the histone H3 acetylation level of *FLC*, *MAF4*, and *MAF5*. As shown in Figure 3, hyperacetylation of histone H3 was found in the first exon and first intron regions of *FLC* and *MAF4* as well as in the first exon of *MAF5*, suggesting that *HDA6* might regulate the expression of these genes by chromatin deacetylation.

Another flowering-autonomous pathway mutant, *fld*, was also shown to have increased histone acetylation levels at the *FLC* locus (He et al., 2003). The T-DNA insertion mutant line from the SAIL T-DNA collection (SAIL_642_C05.v2), *fld-6*, carries a T-DNA insertion in the second exon of *FLD* (Jin et al., 2008). We determined flowering time of *axe1-5*, *fld-6*, and *axe1-5/fld-6* double mutants under both LD and SD conditions (Fig. 4, A and B). *fld-6* mutants flowered much later than *axe1-5* mutants under LD conditions. *axe1-5/fld-6* double mutants flowered later than both *axe1-5* and *fld-6* single mutants, suggesting that *HDA6*

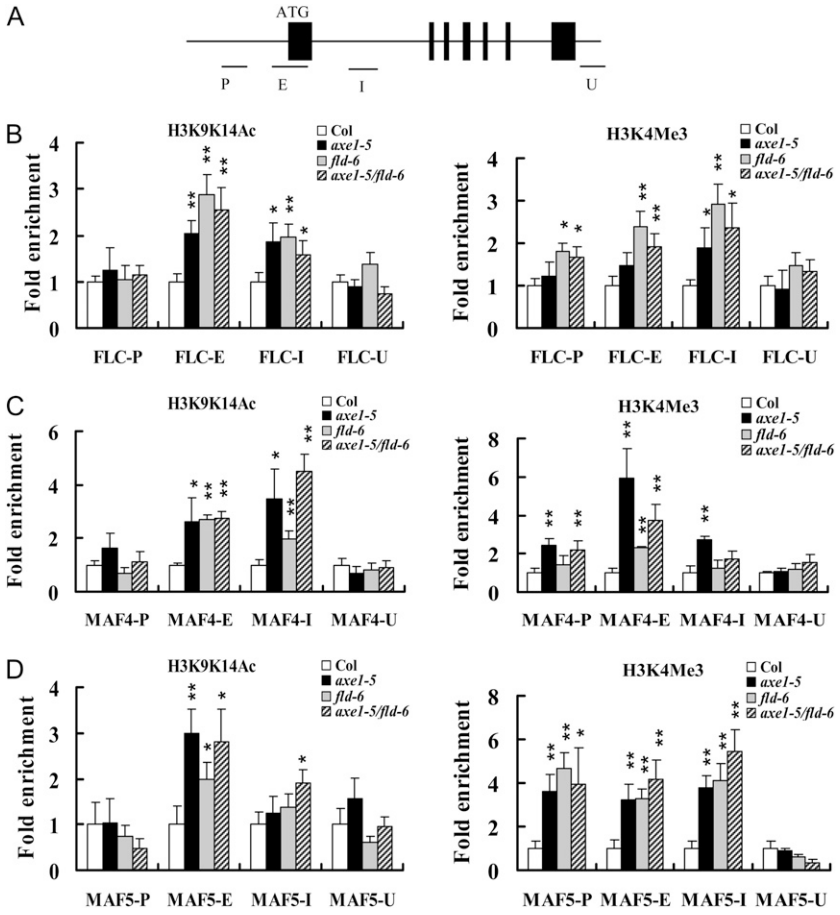

Figure 3. Levels of H3K9K14Ac and H3K4Me3 in *FLC*, *MAF4*, and *MAF5* chromatin. A, Schematic structure of genomic sequences of *FLC*, *MAF4*, and *MAF5* and the regions examined by ChIP. *FLC*, *MAF4*, and *MAF5* have a similar genomic structure, and black boxes represent exons. B to D, Relative levels of H3K9K14Ac and H3K4Me3 in *FLC* (B), *MAF4* (C), and *MAF5* (D) in Col, *axe1-5*, *fld-6*, and *axe1-5/fld-6* seedlings grown under LD conditions for 10 d. The amounts of DNA after ChIP were quantified and normalized to an internal control (*ACTIN2*). The fold enrichments of *axe1-5*, *fld-6*, and *axe1-5/fld-6* over Col at the indicated regions are shown. The values shown are means ± SD. * $P < 0.05$, ** $P < 0.01$.

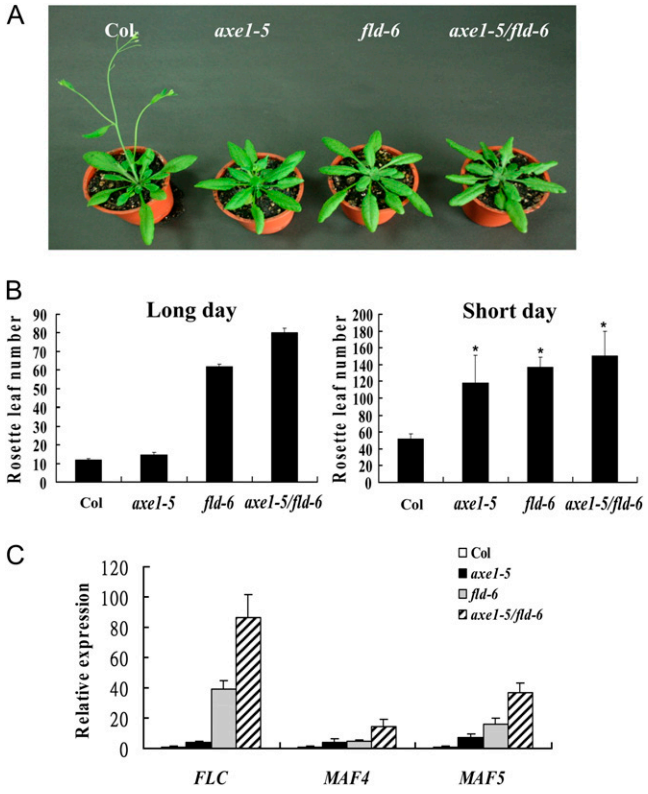

Figure 4. Phenotypes of *axe1-5*, *fld-6*, and *axe1-5/fld-6*. A, *axe1-5*, *fld-6*, and *axe1-5/fld-6* plants grown under LD conditions compared with the Col wild type. B, Rosette leaf numbers at bolting of Col, *axe1-5*, *fld-6*, and *axe1-5/fld-6* plants grown under LD and SD conditions. Error bars indicate SD. At least 20 plants were scored for each line. * Some *axe1-5* plants and all of the *fld-6* and *axe1-5/fld-6* plants did not flower 220 d after germination, and the rosette leaf number was counted at 220 d. C, qRT-PCR analysis of the expression of *FLC*, *MAF4*, and *MAF5* in Col, *axe1-5*, *fld-6*, and *axe1-5/fld-6* plants grown under LD conditions for 20 d. The values shown are means ± SD. [See online article for color version of this figure.]

and *FLD* may independently regulate flowering in an additive way. We compared the expression of *FLC*, *MAF4*, and *MAF5* in *axe1-5*, *fld-6*, and *axe1-5/fld-6* plants by quantitative reverse transcription (qRT)-PCR. As shown in Figure 4C, we observed the higher expression of *FLC*, *MAF4*, and *MAF5* in *axe1-5*, *fld-6*, and *axe1-5/fld-6* plants compared with wild-type ecotype Columbia (Col) plants. In addition, the *FLC* transcript level of *fld-6* plants was higher than that of *axe1-5* plants, whereas *axe1-5/fld-6* plants displayed the highest level of *FLC* expression, which is consistent with their phenotype difference in flowering time.

We compared the histone H3 acetylation levels of *fld-6* and the double mutant *axe1-5/fld-6* with that of *axe1-5*. Hyperacetylation of histone H3 was found in the first exon and first intron regions of *FLC* and *MAF4* as well as in the first exon of *MAF5* in *axe1-5*, *fld-6*, and *axe1-5/fld-6* (Fig. 3, B–D). These results indicate that both HDA6 and FLD may regulate *FLC*, *MAF4*, and *MAF5* expression by histone acetylation during the transition switch from the vegetative stage to reproductive development. We also analyzed H3K4 trimethylation levels of *FLC*, *MAF4*, and *MAF5* in *axe1-5* and *fld-6* plants. Increased H3K4 trimethylation was found in the first intron region of *FLC*, the first exon of *MAF4*, and all three regions of *MAF5* in *axe1-5*, *fld-6*, and *axe1-5/fld-6* (Fig. 3, B–D).

Interaction of HDA6 and FLD

A yeast two-hybrid assay was used to examine whether there is a direct protein interaction between FLD and HDA6. It was found that the full-length FLD interacted with the C-terminal region (amino acids 333–471) of HDA6 (Fig. 5A); this region is characterized by high Asp content. Further analysis indicated that the C-terminal region of HDA6 interacted with the FLD N-terminal region (Fig. 5B) that contains a SWI3P, Rsc8p, and Moira (SWIRM) domain (Aravind and Iyer, 2002). These results suggest that FLD can directly interact with HDA6, and the SWIRM domain in the N-terminal region of FLD and the C-terminal region of HDA6 are responsible for the interaction between these two proteins. FLD contains a SWIRM domain that is found in many chromosomal proteins involved in chromatin modifications or remodeling (Qian et al., 2005). The interaction of FLD amino acids 1 to 168 with the HDA6 C-terminal region suggests that the SWIRM

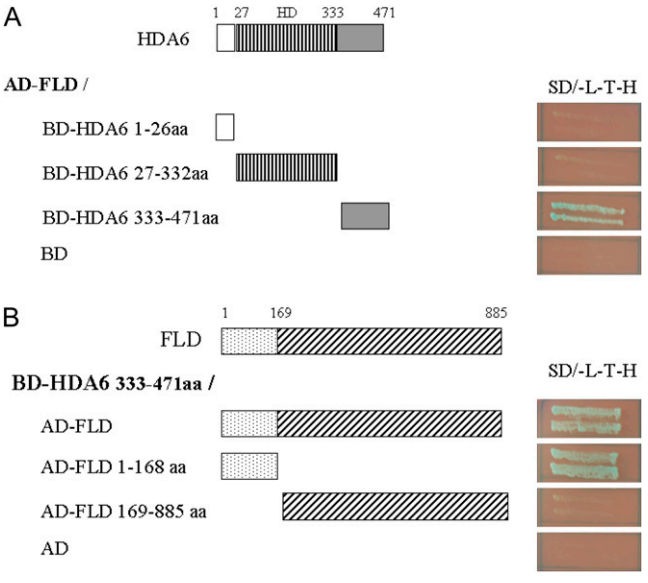

Figure 5. HDA6 interacted with FLD in yeast two-hybrid assays. A, Different regions of HDA6 fused with the Gal4 binding domain (BD) and the full-length FLD fused with the Gal4 activation domain (AD) were cotransformed into the yeast strain AH109. B, Different regions of FLD fused with AD and the C-terminal fragment of HDA6 fused with BD were cotransformed into the yeast strain AH109. The transformants were plated onto plates with SD/-Leu-Trp-His/3-amino-1,2,4-triazole/5-bromo-4-chloro-3-indolyl-α-D-galactopyranoside for 3 d. aa, Amino acids. [See online article for color version of this figure.]

domain might act as an important link among chromatin-remodeling proteins.

BiFC was used to further determine the interaction between HDA6 and FLD. Both HDA6 and FLD were fused to the N-terminal 174-amino acid portion of yellow fluorescent protein (YFP) in the pEarleyGate201 vector (pEarleyGate201-YN) as well as the C-terminal 66-amino acid portion of YFP in the pEarleyGate202 vector (pEarleyGate202-YC; Lu et al., 2010). The corresponding constructs were codelivered into protoplasts of Arabidopsis, and fluorescence was observed using a confocal microscope. As shown in Figure 6A, yellow fluorescence was observed at the nuclear periphery when HDA6-YC was cotransformed with FLD-YN. Similar results were also observed when HDA6-YN was cotransformed with FLD-YC (Supplemental Fig. S1). These data indicate that HDA6 interacts with FLD and that the interaction site is at the nuclear periphery. Recent studies suggest that the peripheral zone of the nucleus is the area associated with the regulation of gene expression, especially gene silencing (Deniaud and Bickmore, 2009).

The interaction between HDA6 and FLD was further analyzed by in vitro pull-down and coimmunoprecipitation assays. For in vitro pull-down assay, purified FLD-His recombinant protein was incubated with glutathione *S*-transferase (GST)-HDA6 protein. As shown in Figure 6B, FLD-His was pulled down by GST-HDA6. Similarly, GST-HDA6 was also pulled down by FLD-His. These results indicate that HDA6 is directly associated with FLD. For coimmunoprecipitation assay, a tobacco (*Nicotiana benthamiana*) transient expression system was used (Yang et al., 2008). Tobacco leaves were infiltrated with *Agrobacterium* cultures carrying *35S:GFP-HDA6* and *35S:Myc-FLD*, and leaf extracts were analyzed by coimmunoprecipitation. As shown in Figure 6C, GFP-HDA6 was coimmunoprecipitated by Myc-FLD. The interaction was specific, as GFP-HDA6 was not detected in the absence of Myc-FLD.

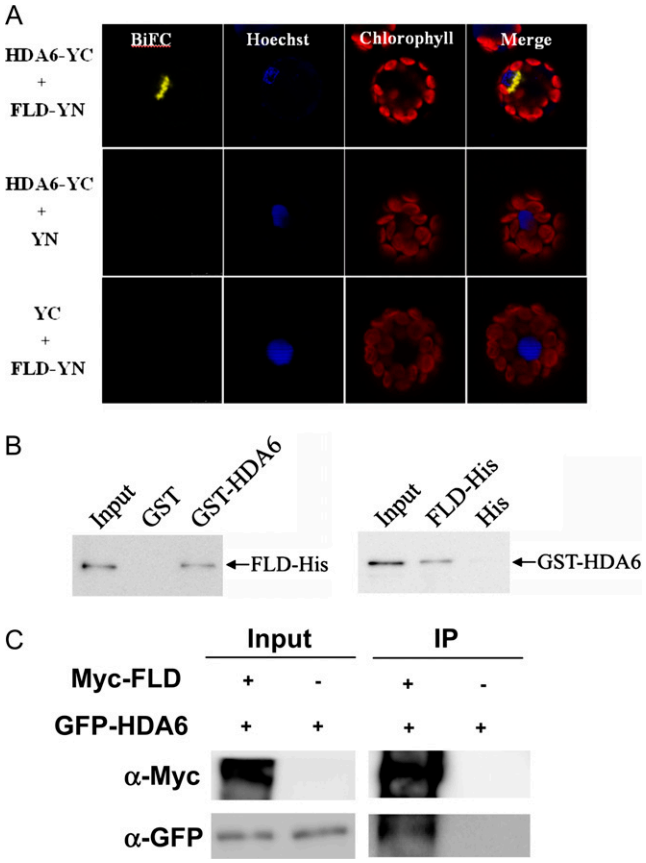

Figure 6. HDA6 physically interacted with FLD. A, BiFC in Arabidopsis protoplasts showing interaction between HDA6 and FLD in living cells. HDA6 and FLD fused with the N terminus (YN) or the C terminus (YC) of YFP were cotransfected into protoplasts and visualized using confocal microscopy. As a negative control, HDA6 and FLD fused with YN or YC and empty vectors (YN and YC) were cotransfected into protoplasts. B, HDA6 interacted with FLD in a pull-down assay. GST-HDA6 or GST was incubated with FLD-His and GST affinity resin, and the bound proteins were then eluted from resin and probed with the anti-His antibody (left panel). FLD-His or His was incubated with GST-HDA6 and His affinity resin, and the bound proteins were then eluted from resin and probed with the anti-GST antibody (right panel). C, In vivo interaction between HDA6 and FLD in tobacco. *Agrobacterium* cultures carrying 35S:GFP-HDA6 and 35S:Myc-FLD were coinfiltrated into tobacco leaves. Transiently expressed GFP-HDA6 and Myc-FLD were analyzed by coimmunoprecipitation. Crude extracts (input) were immunoprecipitated (IP) with an anti-Myc antibody and analyzed by western blotting.

Genome-Wide Transcriptomic Analysis of *HDA6*-RNAi Plants

We compared the gene expression profiles of the *HDA6*-RNAi plants (cs24039) and ecotype Wassilewskija (Ws) wild-type plants by using Affymetrix microarray. Total RNA was isolated from rosette leaves of 3-week-old plants growing under SD conditions (16 h of dark and 8 h of light). Three independent biological samples were used to do microarray analysis, and microarray data were analyzed by the National Institute of Aging Array analysis software (Sharov et al., 2005). Those genes identified by 2-fold filtered increase or decrease and with $P \leq 0.05$ were considered to have significant expression differences. Compared with Ws, 441 genes were up-regulated but only 46 genes were down-regulated in *HDA6*-RNAi plants (Supplemental Tables S3 and S4), supporting the generally accepted idea that a HDAC acts mainly as a transcriptional repressor. Those genes affected by HDA6 are involved in a variety of biological processes (Supplemental Fig. S2). In particular, 9% of genes are involved in developmental processes, including flowering regulation, 5% of genes are involved in gene silencing, and 12% of genes are involved in stress response (Supplemental Fig. S2).

The microarray analysis revealed that a number of genes involved in flowering were up- or down-regulated in *HDA6*-RNAi plants (Table I). The cs24039 *HDA6*-RNAi line was previously shown to display a

Table I. *Selected genes affected by HDA6 in microarray analysis*

Gene Name	Arabidopsis Genome Initiative Code	Ratio[a]	*P*	Description
Genes involved in flowering				
MAF4[b]	AT5G65070	12.2	1.00E-05	MADS box protein, negative regulator of flowering
FLC[b]	AT5G10140	8.6	1.00E-05	MADS box protein, negative regulator of flowering
MAF5[b]	AT5G65080	7.6	1.30E-03	MADS box protein, negative regulator of flowering
AGP24[b]	AT5G40738	6.2	1.00E-05	Most highly expressed in pollen
AT1G52000	AT1G52000	3.5	1.00E-05	Flower development
AT5G38440	AT5G38440	3.5	4.90E-02	Self-incompatibility protein relative
AT3G17010	AT3G17010	3.4	1.40E-03	Expressed in stamen primordia
OPR3	AT2G06050	3.2	1.00E-04	Male sterile and pollen dehiscence
ARPN	AT2G02850	2.3	3.00E-04	Involved in anther development and pollination
SMZ[b]	AT3G54990	2.3	1.00E-05	AP2 domain transcription factor
UNE18	AT5G02100	2.3	1.00E-05	Double fertilization forming
MBP2	AT1G52030	2.1	1.00E-04	Flower development
AGL8[b]	AT5G60910	−3.2	5.00E-04	Positive regulation of flower development
SPL5	AT3G15270	−2.5	1.40E-03	Involved in regulation of flowering
SOC1[b]	AT2G45660	−2.4	1.25E-02	Promotes flowering
FT[b]	AT1G65480	−2.3	1.10E-03	Promotes flowering
AT1G04770	AT1G04770	−2.1	1.00E-05	Male sterility MS5 family protein
HAT2	AT5G47370	−1.8	1.40E-03	Homeobox-Leu zipper genes
Genes involved in gene silencing				
AGO5[b]	AT2G27880	12.4	4.30E-03	Similar to AGO1 (ARGONAUTE1)
AGO3[b]	AT1G31290	5.8	3.80E-03	Similar to AGO2 (ARGONAUTE2)
HIS1-3[b]	AT2G18050	3.7	1.00E-05	HISTONE ^{1}H-3
AT1G16705[b]	AT1G16705	3.5	1.73E-02	P300/CBP acetyltransferase-related protein
AT5G64572	AT5G64572	2.4	1.00E-04	Potential natural antisense gene
AT1G63080[b]	AT1G63080	2.3	2.50E-02	Transacting siRNA-generating locus
DMT7[b]	AT5G14620	2.1	3.69E-02	Putative DNA methyltransferase
AT4G08590[b]	AT4G08590	2.1	3.00E-03	Similar to VIM1
AT2G33815	AT2G33815	−2.6	7.00E-04	Potential natural antisense gene
Transposons				
AT5G59620[b]	AT5G59620	25.8	1.00E-05	CACTA-like transposase family
AT2G04770[b]	AT2G04770	16.1	1.00E-05	CACTA-like transposase family
AT5G30450	AT5G30450	9.4	5.00E-04	CACTA-like transposase family
AT5G19015[b]	AT5G19015	6.7	3.10E-03	CACTA-like transposase family
AT3G29650	AT3G29650	4	4.63E-02	CACTA-like transposase family
AT4G09480[b]	AT4G09480	12.7	1.00E-05	Copia-like retrotransposon family
AT2G20460[b]	AT2G20460	6.6	3.00E-04	Copia-like retrotransposon family
AT4G09540[b]	AT4G09540	6.1	2.97E-02	Copia-like retrotransposon family
AT2G11140	AT2G11140	5.7	4.85E-02	Copia-like retrotransposon family
AT2G26630[b]	AT2G26630	8.6	7.00E-04	Transposase IS4 family protein
AT1G42705[b]	AT1G42705	6.5	2.24E-02	hAT-like transposase family
AT2G04460[b]	AT2G04460	40.8	1.00E-04	Similar to pol polyprotein
AT1G47860	AT1G47860	3.8	3.11E-02	Non-LTR retrotransposon family
AT4G03790	AT4G03790	3	1.60E-03	Gypsy-like retrotransposon family
Genes related to stress				
TET9[b]	AT4G30430	8.1	1.00E-04	Involved in aging
AT3G10200[b]	AT3G10200	6.6	3.50E-02	Dehydration-responsive protein-related
AT2G29500[b]	AT2G29500	3.3	1.00E-05	Class I small heat shock protein (HSP17.6B-CI)
SRG1[b]	AT1G17020	3.1	2.64E-02	Senescence-related gene
ATCLH1[b]	AT1G19670	2.3	2.74E-02	Chlorophyll degradation and response to stress
ADR1[b]	AT1G33560	2.3	1.00E-05	Encodes a NBS-LRR disease resistance protein
AOC1[b]	AT3G25760	2.2	3.15E-02	JA biosynthesis
ATCXE18	AT5G23530	2.2	1.98E-02	Similar to ATGID1C/GID1C
JAZ7[b]	AT2G34600	−5.1	1.20E-03	JA signaling
STZ[b]	AT1G27730	−3.9	9.00E-04	Salt tolerance
RHL41[b]	AT5G59820	−3.2	1.41E-02	Cold stress
CBF1	AT4G25490	−2.7	1.40E-03	Cold stress
CBF2	AT4G25470	−3.1	1.00E-04	Cold stress
Transcription factors				
AT1G59930[b]	AT1G59930	17.3	1.00E-05	MADS box protein

(*Table continues on following page.*)

Table I. (*Continued from previous page.*)

Gene Name	Arabidopsis Genome Initiative Code	Ratio[a]	*P*	Description
AGL37[b]	AT1G65330	13.3	1.00E-05	Type 1 MADS box protein
AT2G36080[b]	AT2G36080	3.9	3.17E-02	B3 DNA-binding domain transcription factor
AT3G53370[b]	AT3G53370	3.5	1.00E-04	DNA-binding S1FA family protein
AT5G66980[b]	AT5G66980	3.3	1.00E-05	Transcriptional factor B3 family protein
AT5G25810[b]	AT5G25810	2.4	2.06E-02	ERF/AP2 transcription factor family
AT1G74930[b]	AT1G74930	−7.2	1.00E-05	A member of the DREB subfamily A-5 of ERF/AP2
AT5G61600[b]	AT5G61600	−4	4.00E-04	Encodes a member of the ERF
AT5G51190[b]	AT5G51190	−3	2.70E-02	Encodes a member of the ERF

[a]Expression fold increase or decrease in *HDA6*-RNAi (cs24039) relative to the Ws wild type. [b]Confirmed by quantitative real-time PCR.

similar phenotype as compared with the *axe1-5* mutant (Wu et al., 2008). We further used qRT-PCR to confirm the expression of those genes identified by microarray in *HDA6*-RNAi (cs24039) as well as *axe1-5* plants. Eight genes related to flowering were analyzed by qRT-PCR, and all of them showed a correlation between qRT-PCR and microarray data in both *HDA6*-RNAi and *axe1-5* plants (Fig. 7A). As expected, the expression of the floral repressors *FLC*, *MAF4*, and *MAF5* was up-regulated, whereas the expression of the floral activators *FT* and *SOC1* was down-regulated. In addition to *FLC*, *MAF4*, and *MAF5*, two additional MADS box genes, *AGL37* and *AT1G59930*, were also up-regulated in *axe1-5* and *HDA6*-RNAi plants.

HDA6 is implicated in gene silencing and stress responses (Aufsatz et al., 2007; Wu et al., 2008). Therefore, we investigated the expression of genes related to gene silencing and stress responses by qRT-PCR. Seven genes related to gene silencing were analyzed, and all of them showed a correlation between qRT-PCR and microarray data (Fig. 7B). It is interesting that the expression of two genes encoding AGO proteins, *AGO5* and *AGO3*, was up-regulated. Ten genes involved in stress responses analyzed by qRT-PCR were also shown to be consistent with the microarray data (Fig. 7C). In addition, a subset of transposons was up-regulated in *axe1-5* and *HDA6*-RNAi plants (Table I), supporting a role of *HDA6* in maintaining the stability of transposons (Aufsatz et al., 2007). Nine transposons analyzed all showed a correlation between qRT-PCR and microarray data (Fig. 6D).

Most of the genes identified by DNA microarrays may not be the direct target genes regulated by HDA6. In order to identify the direct targets of HDA6, Arabidopsis plants overexpressing *HDA6*-GFP (*35S*:*HDA6-GFP*) were used to perform the ChIP assay. Overexpressing *35S*:*HDA6-GFP* in the *axe1-5* mutant can complement the delayed-flowering phenotype, suggesting that the HDA6-GFP fusion protein is functional. Real-time PCR was used to determine whether promoters and regions surrounding the translational starting sites of selected genes were enriched by ChIP with an anti-GFP antibody. Among 47 genes tested, HDA6 was recruited to the promoters and/or regions surrounding the translational starting sites of eight genes, *AT1G59930*, *FLC*, *MAF4*, *AGO5*, *AGO3*,

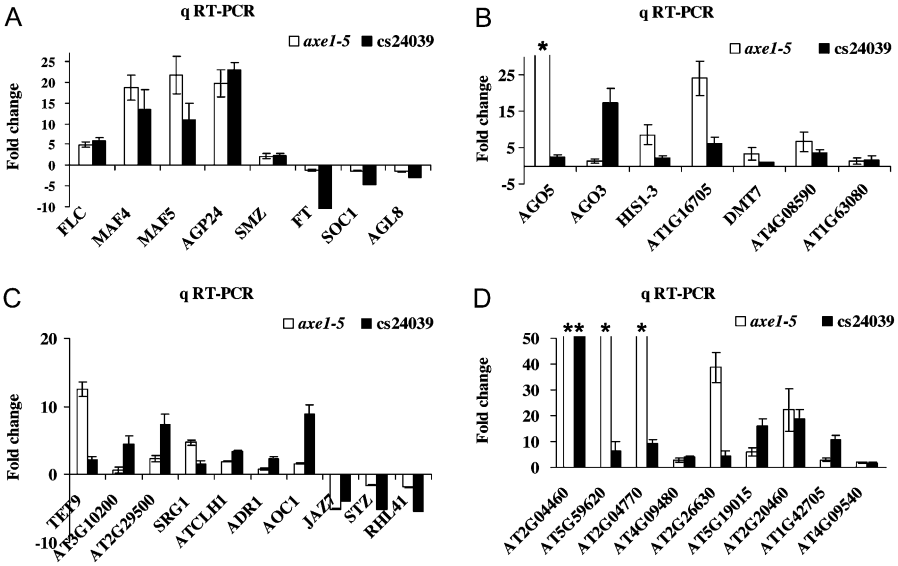

Figure 7. Validation of the DNA microarray data. qRT-PCR analysis of the gene expression involved in flowering (A), gene silencing (B), stress (C), and transposons (D) is shown. Total RNA was isolated from Ws, *HDA6*-RNAi (cs24039), Col, and *axe1-5* plants grown in SD conditions. The values shown are relative fold changes compared with Col (for *axe1-5*) or Ws (for *HDA6*-RNAi) with SD. * The fold change was higher than 20.

AT3G26480, *AT5G66980*, and *AT2G36080* (Fig. 8), suggesting that these genes probably are the direct targets of HDA6.

Genes Up-Regulated in *axe1-5* Plants Are Hyperacetylated

We further investigated histone acetylation levels of the genes affected by HDA6 in the *axe1-5* mutant by ChIP assay. The relative enrichment of histone H3 acetylation was determined by real-time PCR using primers specific for the proximal promoters (within 500 bp upstream of the translation starting sites) and the first exons surrounding the translation start sites of individual genes. Among those up-regulated genes related to flowering, the hyperacetylation of the first exons was found in *FLC*, *MAF4*, *MAF5*, and *AGP24* but not in *SMZ* in *axe1-5* mutants (Fig. 9A). Similar acetylation patterns were also observed in the promoter regions (data not shown). In contrast, there was no significant difference between Col wild-type and *axe1-5* mutant plants in those genes that were down-regulated, such as *FT*, *SOC1*, and *AGL8* (Fig. 9A). The H3K4 trimethylation levels of flowering-related genes were also analyzed. Increased H3K4 trimethylation was found in *AGL37*, *FLC*, *MAF4*, *MAF5*, and *AGP24* in *axe1-5* as well as *fld-6* and *axe1-5/fld-6* plants (Supplemental Fig. S3), suggesting that there is a correlation between histone H3 acetylation and H3K4 trimethylation. These data indicate that HDA6 and FLD may affect similar genes involved in flowering.

We also investigated the histone acetylation of genes related to gene silencing and stress responses as well as transposons by ChIP assay. All of the up-regulated genes related to gene silencing showed hyperacetylation of histone H3 in *axe1-5* (Fig. 9B). Five up-regulated genes involved in stress responses, *TET9*, *SRG1*, *ADR1*, *AT2G29500*, and *AT3G10200*, showed increased histone H3 acetylation in *axe1-5* plants (Fig. 9C). ChIP assay also shows hyperacetylation of histone H3 in the transposons up-regulated in *axe1-5* (Fig. 9D). These data suggest that the up-regulation of gene expression in *axe1-5* mutants was associated with histone hyperacetylation.

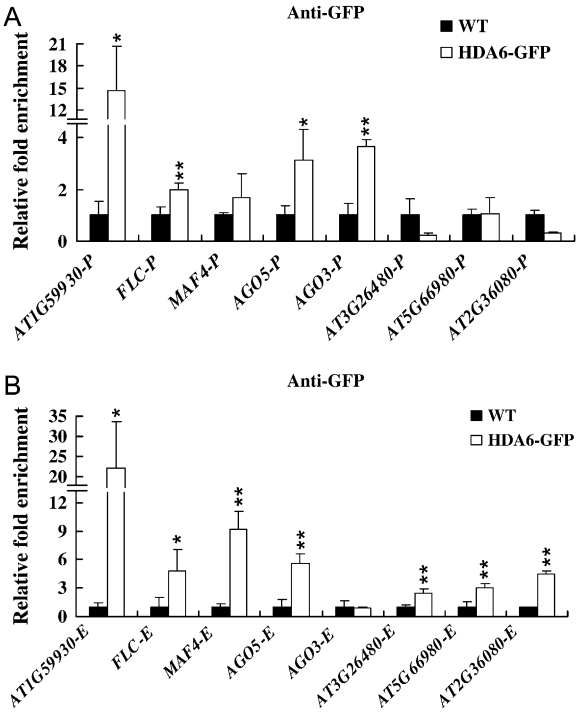

Figure 8. Target genes of HDA6 identified by ChIP followed by real-time PCR analysis. Transgenic plants expressing HDA6-GFP were subjected to ChIP analysis using an anti-GFP antibody. Wild-type (WT) plants were used as negative controls. The relative fold enrichment of a target in the promoter (A) and transcription start site (B) was calculated by dividing the amount of DNA immunoprecipitated from HDA6-GFP transgenic plants by that from the negative control plants and compared with input DNA. * $P < 0.05$, ** $P < 0.01$.

DISCUSSION

Molecular genetic studies on the mechanism of flowering in Arabidopsis have revealed four major flowering pathways: the photoperiod, autonomous, vernalization, and gibberellin pathways (Boss et al., 2004; Henderson and Dean, 2004). The Arabidopsis autonomous floral promotion pathway promotes flowering independently of the photoperiod and vernalization pathways by repressing *FLC* (Michaels and Amasino, 2001). The flowering of *axe1-5* plants was delayed in both LD and SD conditions, and the delay in flowering time of *axe1-5* was completely corrected by vernalization, suggesting that HDA6 is involved in the autonomous pathway of flowering (Wu et al., 2008). We observed that *FLC* was up-regulated and hyperacetylated in *axe1-5* plants. Furthermore, the late-flowering phenotype of *axe1-5* mutants was suppressed by an *flc* null mutant. These data suggest that HDA6 is involved in flowering by regulating *FLC* expression. In addition to *FLC*, *MAF4* and *MAF5* were also up-regulated and hyperacetylated in *axe1-5* plants. By using microarray analysis, two additional MADS box genes, *AGL37* and *AT5G59930*, were also identified to be up-regulated and hyperacetylated in *axe1-5* plants. Since HDA6 is a trichostain A-sensitive histone deacetylase capable of removing acetyl groups from multiple Lys residues of histones (Earley et al., 2006, 2010), HDA6 may repress *FLC* as well as other MADS box genes through deacetylating their chromatin. ChIP analysis indicated that HDA6 bound directly to the promoters of *FLC*, *MAF4*, and *AT5G59930*, suggesting that they may be the direct targets of HDA6. In addition to the increase of *FLC* expression, a portion of the late-flowering phenotype of *axe1-5* mutants could be due to other floral repressors, because *axe1-5/flc-3* double-mutant plants flowered later than *flc-3* single mutant plants.

A large number of mutants have been identified to be involved in the autonomous pathway (Michaels,

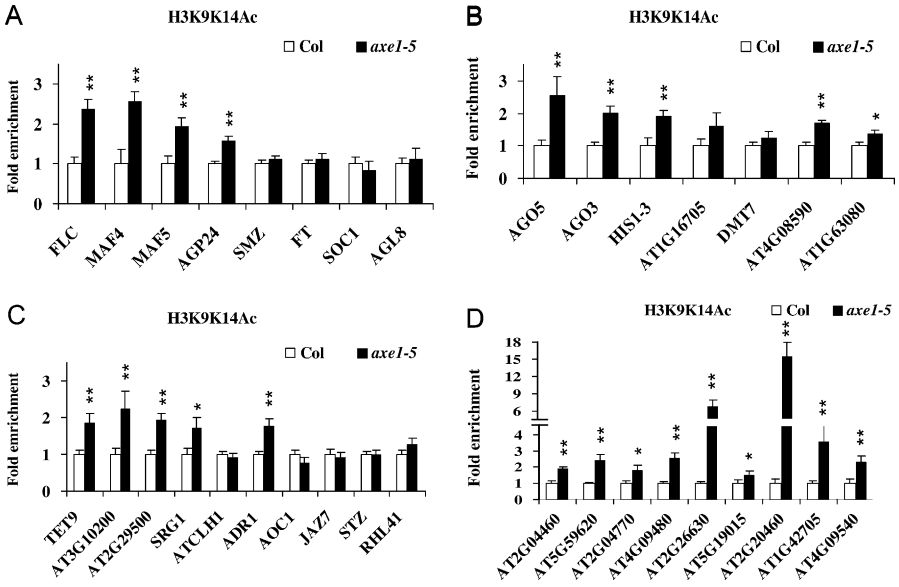

Figure 9. Histone acetylation of genes upregulated in *axe1-5* plants. The relative levels of acetyl H3K9K14 of genes involved in flowering (A), gene silencing (B), stress (C), and transposons (D) in Col and *axe1-5* were analyzed by ChIP. The immunoprecipitated DNA was quantified by real-time PCR and subsequently normalized to an internal control (*ACTIN2*). The fold enrichment of *axe1-5* over Col is shown, and the values shown are means ± SD. * $P < 0.05$, ** $P < 0.01$.

2009). In two autonomous mutants, *fld* and *fve*, *FLC* displays hyperacetylation of histone H3 and H4, indicating that FVE and FLD are required to deacetylate *FLC* chromatin and repress its expression (He et al., 2003; Ausín et al., 2004; Kim et al., 2004). *FVE* encodes the nuclear WD-repeat protein, AtMSI4, a retinoblastoma-associated protein that functions in the histone deacetylase complexes (Ausín et al., 2004; Kim et al., 2004). Hence, FVE is likely to act in a HDAC complex to repress *FLC* expression (Ausín et al., 2004; Kim et al., 2004). *FLD* encodes a plant homolog of mammalian LSD1 and is involved in the H3K4 demethylation and deacetylation of *FLC* chromatin (Jiang et al., 2007; Liu et al., 2007). *axe1-5* and *fld-6* mutants displayed increased levels of H3 acetylation and H3K4 trimethylation in *FLC*, *MAF4*, and *MAF5*, suggesting that both HDA6 and FLD are required for removing H3 acetylation and H3K4 methylation. Compared with the single mutants, the *axe1-5/fld-6* double mutant shows additive effects on *FLC*, *MAF4*, and *MAF5* expression as well as flowering time. However, H3K9K14 acetylation and H3K4 trimethylation levels in the double mutant are similar to those in the single mutants. These data suggest that the enhanced *FLC* expression and delayed flowering time in the double mutant may be caused by factors other than H3K9K14Ac and H2K4Me3.

Although cross talk between histone deacetylation and demethylation has previously been suggested to modulate gene expression in mammalian cells (Shi et al., 2005; Lee et al., 2006), the direct association of a HDAC with a histone demethylase has not been reported. In this study, we found that HDA6 physically associates with FLD in vitro and in vivo, indicating that these two proteins act in the same protein complex. BiFC assays indicate that the interaction site of HDA6 and FLD is at the nuclear periphery. The peripheral zone of the nucleus is the area that has been implicated in the regulation of gene expression, especially gene silencing (Deniaud and Bickmore, 2009). The mammalian histone demethylase, LSD1, is an integral component of histone deacetylase corepressor complexes, in which HDACs and LSD1 may cooperate to remove activating acetyl and methyl histone modifications (Shi et al., 2005; Lee et al., 2006). HDAC inhibitors can diminish histone demethylation activity, whereas the abrogation of LSD1 activity by mutations can decrease deacetylation activity (Lee et al., 2006), suggesting that the enzymatic activities of HDACs and LSD1 are closely linked. Further research is required to determine whether there is a synergistic interplay between histone demethylase and deacetylase activities in plants.

Vernalization also promotes flowering by repressing *FLC* expression (Amasino, 2004; Schmitz and Amasino, 2007). The levels of acetylation of histone H3 at Lys-9 and Lys-14 are reduced during vernalization, followed by an increase in methylation of histone H3 at Lys-9 and Lys-27 (Bastow et al., 2004; Sung and Amasino, 2004). During prolonged cold, VRN5 and VIN3 form a heterodimer necessary for establishing the vernalization-induced chromatin modifications, including histone deacetylation and H3 K27 trimethylation, required for the epigenetic silencing of *FLC* (Greb et al., 2007; De Lucia et al., 2008). VRN5 and VIN3 are members of PHD finger-containing proteins, which are often found in various components of chromatin-remodeling complexes, including HDACs (Aasland et al., 1995; Xia et al., 2003). These observations suggest that HDACs also play an important role in the epigenetic modification directed by vernalization. Since *axe1-5* mutants exhibit a normal vernalization response, HDA6-mediated deacetylation is not required for vernalization (Wu et al., 2008). A recent study suggests that vernalization-mediated FLC repression is via a novel pathway involving the SIR2 class of HDACs, SRT1 and SRT2 (Bond et al., 2009).

axe1 and other mutant alleles of *hda6*, *rts1* and *sil1*, were isolated based on deregulated expression of transgenes (Murfett et al., 2001; Aufsatz et al., 2002; Probst et al., 2004). Mutations in *HDA6* result in the loss of transcriptional silencing from several repetitive transgenic and endogenous templates. Genome-wide gene expression analysis using the Affymetrix GeneChip indicates that down-regulation of *HDA6* affected genes involved in a variety of biological processes. In addition to genes involved in flowering, genes involved in gene silencing and stress responses were also affected in *hda6* mutants, supporting multiple functions of HDA6 (Aufsatz et al., 2007; Wu et al., 2008; Chen et al., 2010; Earley et al., 2010). We found that the expression of two genes encoding AGO proteins, *AGO5* and *AGO3*, was up-regulated in *hda6* mutants. ChIP analysis indicated that HDA6 bound directly to the promoters of *AGO5* and *AGO3*, suggesting that they may be the direct targets of HDA6. The AGO proteins are involved in RNA-silencing processes that also involve 21- to 25-nucleotide short RNAs cleaved from double-stranded RNAs by the RNaseIII enzyme Dicer (Baumberger and Baulcombe, 2005). It is suggested that HDA6 plays an important role in RNAi-mediated heterochromatin formation (Aufsatz et al., 2007; Earley et al., 2010). Up-regulation of *AGO5* and *AGO3* in *hda6* mutants suggests that HDA6 may be involved in RNAi-mediated gene silencing by regulating the expression of *AGO*-like genes.

A subset of transposons was up-regulated in *HDA6*-RNAi and *axe1-5* plants. Similarly, down-regulation of a SIR2-class HDAC, *OsSRT1*, also results in transposon activation in *OsSRT1*-RNAi rice (*Oryza sativa*) plants (Huang et al., 2007). These results suggest that *HDA6* and other HDACs are required to maintain the stability of transposable elements. Besides histone modifications, DNA methylation is also associated with gene-silencing mechanisms in eukaryotic organisms. Recent studies suggest that HDA6 is required for maintaining cytosine methylation (Aufsatz et al., 2007; Earley et al., 2010). Based on genomic transcriptional analysis, we demonstrate that HDA6 regulates transposon expression. In addition, up-regulation of transposons was associated with a high level of chromatin H3 acetylation in the *axe1-5* mutant, suggesting that HDA6 regulates transposon expression by chromatin deacetylation. These results suggest that HDA6 plays an important role in the interplay between histone deacetylation and DNA methylation in transcriptional regulation.

MATERIALS AND METHODS

Plant Materials

Arabidopsis (*Arabidopsis thaliana*) was grown in growth chambers under LD (16 h of light/8 h of dark) or SD (8 h of light/16 h of dark) conditions. The *hda6* mutant line *axe1-5*, the *HDA6* RNAi line cs24039, and the *FLD* T-DNA insertion mutant *fld-6* (SAIL_642_C05.v2) were used in this study. cs24039 is in the Ws background, whereas *axe1-5* and *fld-6* are in the Col background. *axe1-5* was originally isolated based on deregulated expression of auxin-responsive transgenes (Murfett et al., 2001) and was outcrossed into the Col wild type three times.

qRT-PCR Analysis

Arabidopsis leaves (0.1–0.2 g) were ground with liquid nitrogen in a mortar and pestle and mixed with 1 mL of Trizol Reagent (Invitrogen) to isolate total RNA. One microgram of total RNA was used for the first-strand cDNA synthesis after incubation at 65°C for 10 min. cDNA was synthesized in a volume of 20 μL that contained the Moloney murine leukemia virus reverse transcriptase buffer (Promega), 10 mM dithiothreitol (DTT), 1.5 μM poly(dT) primer, 0.5 mM deoxyribonucleotide triphosphates, 25 units of RNasin RNase inhibitor, and 200 units of Moloney murine leukemia virus reverse transcriptase at 37°C for 1 h.

cDNAs obtained from RT were used as templates to run real-time PCR. The following components were added to a reaction tube: 9 μL of iQ SYBR Green Supermix solution (Bio-Rad), 1 μL of 5 μM specific primers, and 8 μL of the diluted template. Thermocycling conditions were 95°C for 3 min followed by 40 cycles of 95°C for 30 s, 60°C for 30 s, and 72°C for 20 s, with a melting curve detected at 95°C for 1 min, 55°C for 1 min, and detection of the denature time from 55°C to 95°C. Each sample was quantified at least in triplicate and normalized using *Ubiquitin10* as an internal control. The gene-specific primer pairs for qRT-PCR are listed in Supplemental Table S1.

Microarray Analysis

Genome-wide gene expression analysis using the Affymetrix Arabidopsis GeneChip was performed using Ws and *HDA6*-RNAi (cs24039) plants. Total RNA was isolated from leaves of 3-week-old plants growing under SD conditions. cDNA synthesis, labeling, hybridization, and scanning of the DNA chips were carried out at the National Taiwan University Center for Genomic Medicine. Microarray experiments were performed in triplicate biological samples. Microarray Analysis Suite 5.0 (Affymetrix) was used for analysis of the microarray data. The software was also used to determine whether the expression of each gene is present or absent (absolute call) and whether the fold change value represents a genuine change in expression (difference call). The statistics program National Institute of Aging Array analysis (Sharov et al., 2005) was used to identify statistically significant differentially expressed genes.

ChIP Assay

The ChIP assay was carried out as described (Gendrel et al., 2005). Chromatin extracts were prepared from young leaves treated with formaldehyde. The chromatin was sheared to an average length of 500 bp by sonication and immunoprecipitated with specific antibodies, including anti-acetylated histone H3K9K14 (catalogue no. 06-599; Millipore) and anti-trimethyl histone H3K4 (catalogue no. 04-745; Millipore). The DNA cross-linked to immunoprecipitated proteins was analyzed by real-time PCR. Relative enrichments of various regions of *FLC*, *MAF4*, and *MAF5* in *axe1-5*, *fld-6*, and *axe1-5/fld-6* over Col were calculated after normalization to *ACTIN2*. Each of the immunoprecipitations was replicated three times, and each sample was quantified at least in triplicate. The primers used for real-time PCR analysis in ChIP assays are listed in Supplemental Table S2.

Yeast Two-Hybrid Assays

Yeast two-hybrid assays were performed according to the instructions for the Matchmaker GAL4-based two-hybrid system 3 (Clontech). Different regions of *HDA6* and *FLD* cDNA fragments were subcloned into pGADT7 and pGBKT7 vectors. All constructs were transformed into yeast strain AH109 by the lithium acetate method, and yeast cells were grown on a minimal medium/-Leu-Trp according to the manufacturer's instructions (Clontech). Transformed colonies were plated onto a minimal medium/-Leu/Trp-His/5-bromo-4-chloro-3-indolyl-α-D-galactopyranoside containing 0.5 mM 3-amino-1,2,4-triazole to test for possible interactions between FLD and HDA6.

BiFC Assays

To generate the constructs for BiFC, full-length coding sequences of *HDA6* and *FLD* were PCR amplified. The PCR products were subcloned into the

pENTR/SD/D-TOPO or pCR8/GW/TOPO vector and then recombined into the pEarleyGate201-YN and pEarleyGate202-YC vectors (Lu et al., 2010). The resulting constructs were used for transient assays by polyethylene glycol transfection of Arabidopsis protoplasts (Yoo et al., 2007). Transfected cells were imaged using the TCS SP5 Confocal Spectral Microscope Imaging System (Leica).

In Vitro Pull-Down Assay

The pull-down assay was performed as described previously (Yang et al., 2008) with some modifications. For GST pull-down, GST and GST-HDA6 recombinant proteins were incubated with 30 μL of GST resin in a binding buffer (50 mM Tris-Cl, pH 7.5, 100 mM NaCl, 0.25% Triton X-100, and 35 mM β-mercaptoethanol) for 2 h at 4°C, the binding reaction was washed three times with the binding buffer, and then the FLD-His recombinant protein was added and incubated for an additional 2 h at 4°C. For His pull-down, His and FLD-His recombinant proteins were incubated with 30 μL of His resin in a phosphate buffer (10 mM Na_2HPO_4, 10 mM NaH_2PO_4, 500 mM NaCl, and 10 mM imidazole) for 2 h at 4°C, the binding reaction was washed three times with the phosphate buffer, and then GST-HDA6 recombinant protein was added and incubated for an additional 2 h at 4°C. After extensive washing (at least eight times), the pulled down proteins were eluted by boiling, separated by 10% SDS-PAGE, and detected by western blotting using an anti-His or anti-GST antibody.

Coimmunoprecipitation Assay

Coimmunoprecipitation assay was performed as described by Yang et al. (2008). Two days after infiltration, tobacco (*Nicotiana benthamiana*) leaves were harvested and ground in liquid nitrogen. Proteins were extracted in an extraction buffer (50 mM Tris-HCl, pH 7.4, 150 mM NaCl, 2 mM $MgCl_2$, 1 mM DTT, 20% glycerol, and 1% Igepal CA-630 [Sigma-Aldrich]) containing protease inhibitor cocktail (Roche). Cell debris was pelleted by centrifugation at 14,000*g* for 20 min. The supernatant was incubated with 6 μg of anti-Myc antibody (Sigma) for 4 h at 4°C, then 50 μL of protein A agarose beads (Millipore) was added. After 2 h of incubation at 4°C, the beads were centrifuged and washed six times with a washing buffer (50 mM Tris-HCl, pH 7.4, 150 mM NaCl, 2 mM $MgCl_2$, 1 mM DTT, 10% glycerol, and 1% CA-630). Proteins were eluted with 40 μL of 2.5× sample buffer and analyzed by western blotting using anti-GFP and anti-Myc antibodies (Santa Cruz Biotechnologies).

Supplemental Data

The following materials are available in the online version of this article.

Supplemental Figure S1. BiFC in Arabidopsis protoplasts showing interaction between HDA6 and FLD in living cells.

Supplemental Figure S2. Classification of genes affected by HDA6 in the DNA microarray analysis.

Supplemental Figure S3. Histone H3K4 trimethylation of flowering-related genes in *axe1-5*, *fld-6*, and *axe1-5/fld-6* plants.

Supplemental Table S1. Gene-specific primer pairs for qRT-PCR.

Supplemental Table S2. Primers used for real-time PCR analysis in ChIP assays.

Supplemental Table S3. Genes up-regulated in the *HDA6*-RNAi line compared with the wild type.

Supplemental Table S4. Genes down-regulated in the *HDA6*-RNAi line compared with the wild type.

ACKNOWLEDGMENTS

We are grateful to Dr. Jun-Yi Yang for help with the coimmunoprecipitation assay and Dr. Rick M. Amasino for providing *flc-3* seeds.

Received February 14, 2011; accepted March 9, 2011; published March 10, 2011.

LITERATURE CITED

Aasland R, Gibson TJ, Stewart AF (1995) The PHD finger: implications for chromatin-mediated transcriptional regulation. Trends Biochem Sci **20:** 56–59

Amasino R (2004) Take a cold flower. Nat Genet **36:** 111–112

Aravind, L and Iyer, L M. (2002) The SWIRM domain: a conserved module found in chromosomal proteins points to novel chromatin-modifying activities. Genome Biol **3:** research0039.1–research0039.7

Aufsatz W, Mette MF, van der Winden J, Matzke M, Matzke AJ (2002) HDA6, a putative histone deacetylase needed to enhance DNA methylation induced by double-stranded RNA. EMBO J **21:** 6832–6841

Aufsatz W, Stoiber T, Rakic B, Naumann K (2007) Arabidopsis histone deacetylase 6: a green link to RNA silencing. Oncogene **26:** 5477–5488

Ausín I, Alonso-Blanco C, Jarillo JA, Ruiz-García L, Martínez-Zapater JM (2004) Regulation of flowering time by FVE, a retinoblastoma-associated protein. Nat Genet **36:** 162–166

Bastow R, Mylne JS, Lister C, Lippman Z, Martienssen RA, Dean C (2004) Vernalization requires epigenetic silencing of *FLC* by histone methylation. Nature **427:** 164–167

Baumberger N, Baulcombe DC (2005) Arabidopsis ARGONAUTE1 is an RNA Slicer that selectively recruits microRNAs and short interfering RNAs. Proc Natl Acad Sci USA **102:** 11928–11933

Berger SL (2007) The complex language of chromatin regulation during transcription. Nature **447:** 407–412

Bond DM, Dennis ES, Pogson BJ, Finnegan EJ (2009) Histone acetylation, VERNALIZATION INSENSITIVE 3, FLOWERING LOCUS C, and the vernalization response. Mol Plant **2:** 724–737

Boss PK, Bastow RM, Mylne JS, Dean C (2004) Multiple pathways in the decision to flower: enabling, promoting, and resetting. Plant Cell (Suppl) **16:** S18–S31

Chen LT, Luo M, Wang YY, Wu K (2010) Involvement of Arabidopsis histone deacetylase HDA6 in ABA and salt stress response. J Exp Bot **61:** 3345–3353

Chen ZJ, Tian L (2007) Roles of dynamic and reversible histone acetylation in plant development and polyploidy. Biochim Biophys Acta **1769:** 295–307

Clough SJ, Bent AF (1998) Floral dip: a simplified method for Agrobacterium-mediated transformation of *Arabidopsis thaliana*. Plant J **16:** 735–743

De Lucia F, Crevillen P, Jones AM, Greb T, Dean C (2008) A PHD-polycomb repressive complex 2 triggers the epigenetic silencing of FLC during vernalization. Proc Natl Acad Sci USA **105:** 16831–16836

Deng W, Liu C, Pei Y, Deng X, Niu L, Cao X (2007) Involvement of the histone acetyltransferase AtHAC1 in the regulation of flowering time via repression of FLOWERING LOCUS C in Arabidopsis. Plant Physiol **143:** 1660–1668

Deniaud E, Bickmore WA (2009) Transcription and the nuclear periphery: edge of darkness? Curr Opin Genet Dev **19:** 187–191

Dennis ES, Peacock WJ (2007) Epigenetic regulation of flowering. Curr Opin Plant Biol **10:** 520–527

Earley K, Lawrence RJ, Pontes O, Reuther R, Enciso AJ, Silva M, Neves N, Gross M, Viegas W, Pikaard CS (2006) Erasure of histone acetylation by Arabidopsis HDA6 mediates large-scale gene silencing in nucleolar dominance. Genes Dev **20:** 1283–1293

Earley KW, Pontvianne F, Wierzbicki AT, Blevins T, Tucker S, Costa-Nunes P, Pontes O, Pikaard CS (2010) Mechanisms of HDA6-mediated rRNA gene silencing: suppression of intergenic Pol II transcription and differential effects on maintenance versus siRNA-directed cytosine methylation. Genes Dev **24:** 1119–1132

Gendrel AV, Lippman Z, Martienssen R, Colot V (2005) Profiling histone modification patterns in plants using genomic tiling microarrays. Nat Methods **2:** 213–218

Greb T, Mylne JS, Crevillen P, Geraldo N, An H, Gendall AR, Dean C (2007) The PHD finger protein VRN5 functions in the epigenetic silencing of Arabidopsis FLC. Curr Biol **17:** 73–78

He Y, Amasino RM (2005) Role of chromatin modification in flowering-time control. Trends Plant Sci **10:** 30–35

He Y, Michaels SD, Amasino RM (2003) Regulation of flowering time by histone acetylation in *Arabidopsis*. Science **302:** 1751–1754

Helliwell CA, Wood CC, Robertson M, James Peacock W, Dennis ES (2006) The *Arabidopsis* FLC protein interacts directly *in vivo* with SOC1 and FT chromatin and is part of a high-molecular-weight protein complex. Plant J **46:** 183–192

Henderson IR, Dean C (2004) Control of Arabidopsis flowering: the chill before the bloom. Development **131:** 3829–3838

Huang L, Sun Q, Qin F, Li C, Zhao Y, Zhou DX (2007) Down-regulation of a *SILENT INFORMATION REGULATOR2*-related histone deacetylase

gene, *OsSRT1*, induces DNA fragmentation and cell death in rice. Plant Physiol **144:** 1508–1519

Jiang D, Yang W, He Y, Amasino RM (2007) *Arabidopsis* relatives of the human lysine-specific Demethylase1 repress the expression of FWA and FLOWERING LOCUS C and thus promote the floral transition. Plant Cell **19:** 2975–2987

Jin JB, Jin YH, Lee J, Miura K, Yoo CY, Kim WY, Van Oosten M, Hyun Y, Somers DE, Lee I, et al (2008) The SUMO E3 ligase, *AtSIZ1*, regulates flowering by controlling a salicylic acid-mediated floral promotion pathway and through effects on *FLC* chromatin structure. Plant J **53:** 530–540

Kim HJ, Hyun Y, Park JY, Park MJ, Park MK, Kim MD, Kim HJ, Lee MH, Moon J, Lee I, et al (2004) A genetic link between cold responses and flowering time through FVE in *Arabidopsis thaliana*. Nat Genet **36:** 167–171

Lee MG, Wynder C, Bochar DA, Hakimi MA, Cooch N, Shiekhattar R (2006) Functional interplay between histone demethylase and deacetylase enzymes. Mol Cell Biol **26:** 6395–6402

Liu F, Quesada V, Crevillén P, Bäurle I, Swiezewski S, Dean C (2007) The Arabidopsis RNA-binding protein FCA requires a lysine-specific demethylase 1 homolog to downregulate FLC. Mol Cell **28:** 398–407

Lu Q, Tang X, Tian G, Wang F, Liu K, Nguyen V, Kohalmi SE, Keller WA, Tsang EW, Harada JJ, et al (2010) Arabidopsis homolog of the yeast TREX-2 mRNA export complex: components and anchoring nucleoporin. Plant J **61:** 259–270

Michaels SD (2009) Flowering time regulation produces much fruit. Curr Opin Plant Biol **12:** 75–80

Michaels SD, Amasino RM (2001) Loss of FLOWERING LOCUS C activity eliminates the late-flowering phenotype of FRIGIDA and autonomous pathway mutations but not responsiveness to vernalization. Plant Cell **13:** 935–941

Murfett J, Wang XJ, Hagen G, Guilfoyle TJ (2001) Identification of *Arabidopsis* histone deacetylase HDA6 mutants that affect transgene expression. Plant Cell **13:** 1047–1061

Pandey R, Müller A, Napoli CA, Selinger DA, Pikaard CS, Richards EJ, Bender J, Mount DW, Jorgensen RA (2002) Analysis of histone acetyltransferase and histone deacetylase families of Arabidopsis thaliana suggests functional diversification of chromatin modification among multicellular eukaryotes. Nucleic Acids Res **30:** 5036–5055

Probst AV, Fagard M, Proux F, Mourrain P, Boutet S, Earley K, Lawrence RJ, Pikaard CS, Murfett J, Furner I, et al (2004) *Arabidopsis* histone deacetylase HDA6 is required for maintenance of transcriptional gene silencing and determines nuclear organization of rDNA repeats. Plant Cell **16:** 1021–1034

Qian C, Zhang Q, Li S, Zeng L, Walsh MJ, Zhou MM (2005) Structure and chromosomal DNA binding of the SWIRM domain. Nat Struct Mol Biol **12:** 1078–1085

Schmitz RJ, Amasino RM (2007) Vernalization: a model for investigating epigenetics and eukaryotic gene regulation in plants. Biochim Biophys Acta **1769:** 269–275

Sharov AA, Dudekula DB, Ko MS (2005) A Web-based tool for principal component and significance analysis of microarray data. Bioinformatics **21:** 2548–2549

Shi YJ, Matson C, Lan F, Iwase S, Baba T, Shi Y (2005) Regulation of LSD1 histone demethylase activity by its associated factors. Mol Cell **19:** 857–864

Sung S, Amasino RM (2004) Vernalization in *Arabidopsis thaliana* is mediated by the PHD finger protein VIN3. Nature **427:** 159–164

Wu K, Zhang L, Zhou C, Yu CW, Chaikam V (2008) HDA6 is required for jasmonate response, senescence and flowering in Arabidopsis. J Exp Bot **59:** 225–234

Xia ZB, Anderson M, Diaz MO, Zeleznik-Le NJ (2003) MLL repression domain interacts with histone deacetylases, the polycomb group proteins HPC2 and BMI-1, and the corepressor C-terminal-binding protein. Proc Natl Acad Sci USA **100:** 8342–8347

Yang JY, Iwasaki M, Machida C, Machida Y, Zhou X, Chua NH (2008) BetaC1, the pathogenicity factor of TYLCCNV, interacts with AS1 to alter leaf development and suppress selective jasmonic acid responses. Genes Dev **22:** 2564–2577

Yoo SD, Cho YH, Sheen J (2007) Arabidopsis mesophyll protoplasts: a versatile cell system for transient gene expression analysis. Nat Protoc **2:** 1565–1572